

Non-commercial use only.

Binod Joshi, Thomas A. Smith, and Yanhua Shih, "Multi-band interference and imaging via joint-detection of two-photon beats from thermal radiation," Opt. Express 32, 7640-7650 (2024).

<https://doi.org/10.1364/OE.518875>

Access to this work was provided by the University of Maryland, Baltimore County (UMBC) ScholarWorks@UMBC digital repository on the Maryland Shared Open Access (MD-SOAR) platform.

**Please provide feedback**

Please support the ScholarWorks@UMBC repository by emailing [scholarworks-group@umbc.edu](mailto:scholarworks-group@umbc.edu) and telling us what having access to this work means to you and why it's important to you. Thank you.



# Multi-band interference and imaging via joint-detection of two-photon beats from thermal radiation

BINOD JOSHI,\*  THOMAS A. SMITH,  AND YANHUA SHIH

Department of Physics, University of Maryland Baltimore County, Baltimore, Maryland 21250, USA

\*binodjl@umbc.edu

**Abstract:** We present a theoretical discussion of multi-band two-photon interference via joint detection by “slow” detectors and extend it to a technique for multi-band ghost imaging. This technique exploits the advantage of two-photon optical beats over classical optical beats with multi-band thermal light, where the beat frequency can be resolved from intensity fluctuation correlation measurement with two relatively slow photodetectors. The underlying two-photon beats represent a two-photon interference phenomenon: a pair of randomly created and randomly paired photons interfering with the pair itself. A notable implication of the two-photon beats is that they can be turbulence-resistant, which makes our result not only of fundamental interest but also practically useful.

© 2024 Optica Publishing Group under the terms of the [Optica Open Access Publishing Agreement](#)

## 1. Introduction

Two-photon interference, which is a manifestation of quantum correlations in light, has been extensively applied to study both the fundamental understanding of nontrivial optical properties and practical applications [1]. The practical realization of the two-photon interference involves intensity fluctuation correlations (IFC) measurement or joint photodetection by a pair of detectors. Intensity fluctuations in thermal light are proportional to the bandwidth of the source so, due to the relatively slow response time of detectors, it is common to use monochromatic sources for IFC measurements. The use of broadband light sources, such as sunlight or X-ray sources, faces the challenge of “slow” response time of even the state-of-the-art detectors. Optical measurement techniques specifically designed for broadband sources could help in overcoming such challenges. We have found that the use of “multi-band” sources is an attractive tool to build such techniques because of the ability of slow detectors to measure IFC of the individual monochromatic frequency bands.

In this article, we discuss a two-photon interference phenomenon which is able to produce two photon beats from incoherent thermal fields via the joint detection of two relatively slow photodetectors that are unable to follow the beat frequency. For our purpose, we have defined a thermal source with multiple color bands, each with a narrow spectrum, as a “multi-band” source. While the slow detectors are unable to respond to fluctuations from the entire bandwidth of a multi-band source, they are fast enough to respond to fluctuations exclusively from distinct frequency bands. We have found that the intensity fluctuation correlation for the joint detection of incoherent radiation by two slow detectors as a whole is the result of superimposed monochromatic two-photon interference terms. As the *observable* beats result from the superposition of monochromatic two-photon interference and not directly from the interference of bichromatic two-photon amplitudes (which do not survive the time averaging effect of slow detectors), we would like to define such observation as “indirect two-photon beats”. For the purpose of this paper, this is the intended meaning whenever we refer to two-photon beats. In a double-slit interferometer, such superposition results in a measurable *beat frequency*, which, owing to its origin from two-photon interference, is regarded as two-photon beats phenomenon.

One can also extend this concept to a ghost imaging setup based on a multi-band source and describe the point-to-point correlation between the object plane and the imaging plane in terms of these two-photon beats, thus suggesting potential for multi-band imaging.

The observed optical beats are the result of two-photon interference: a pair of randomly created and randomly paired photons interfering with the pair itself [1–4]. To focus on the two-photon interference induced optical beats, we measure the intensity fluctuation correlation (IFC), in lieu of the full second-order correlation function  $G^{(2)}$  [1,5]. For example, in a Young's double-slit interferometer, we shall have two point-like photodetectors,  $D_1$  and  $D_2$ , scannable on the observation plane, followed by an electronic circuit to measure the intensity fluctuation correlation. The light source of the interferometer is assumed to emit incoherent fields of two frequencies (colors) in thermal state, which we have labeled as green (G) and red (R), with a temporal beat frequency  $\omega_{0G} - \omega_{0R}$  much greater than the response frequency of the detectors. In addition, the separation of the double-slit is chosen to be sufficiently greater than the spatial coherence lengths of the two fields,  $d \gg l_c$ , so that no first-order interference (and hence, no first-order optical beats) is observable when  $D_1$  and  $D_2$ , respectively, are scanned along the observation plane of the double-slit interferometer [6]. If, instead, second-order measurement is done on the same setup, an interference pattern is observed with high visibility [1,7–10]. In fact, in the joint measurement of  $D_1$  and  $D_2$ , we are able to observe three two-photon interferences: the two-photon interference as functions of the relative distance between  $D_1$  and  $D_2$  modulated in frequencies  $\omega_{0G}$  and  $\omega_{0R}$ , and sinusoidal beats with frequency  $\omega_{0G} - \omega_{0R}$ . It is interesting to note that the two-photon beats is observable from the joint-measurement of two slow detectors  $D_1$  and  $D_2$  that are unable to respond to  $\omega_{0G} - \omega_{0R}$ .

Another interesting feature is that both the two-photon interference patterns and the two-photon beats, are turbulence-resistant, i.e., any fluctuations in the index of refraction caused by the presence of turbulence in the optical paths of the interferometer do not affect the interference pattern. While it has been established that turbulence has, in general, detrimental effects in interferometry [11,12], turbulence-resistant two-photon interference in a double-slit interferometer has been successfully demonstrated [9,10]. For two-photon interference to remain unaffected by the turbulence, the corresponding two-photon amplitudes should remain spatially overlapped while the radiation field passes through the turbulent medium after emerging from the slits. Such overlap suggests that the detrimental effects of turbulence are canceled out and the observation of second-order interference and, by extension, beats is possible. Recalling the discussion above regarding the role of the two-photon beats in the realization of multi-band ghost imaging, this also implies the turbulence-resistant nature of such imaging scheme.

In this paper, we first present a theoretical framework for the two-photon interference for a multi-band source. For this discussion, we start from a brief introduction of Einstein's granularity picture of radiation. A detailed evaluation of the above mentioned turbulence-resistant two-photon interference will be given based on Einstein's picture. We then extend the multi-band two-photon interference discussion to specific applications of multi-band optical measurement techniques, namely two-photon beats in Young's double-slit interferometer and turbulence-resistant multi-band ghost imaging.

## 2. Einstein's granularity picture

### 2.1. Intensity and intensity fluctuations

In the granularity picture of radiation introduced by Einstein, each atomic transition occurring in a natural source of light will create a "bundle of ray" [13–15]. In our discussion, we will represent each atomic transition by a point-like "sub-source" and each bundle of ray by a microscopic fraction of the total electromagnetic field of the system, called "subfield". This subfield is equivalent to the quantum mechanical concept of a photon; more precisely, it has the same mathematical expression as the effective wavefunction of a photon in thermal state [1,5,16].

The following expression describes the total electric field, consisting of a large number of subfields, measured at a space-time coordinate point  $(\mathbf{r}, t)$ :

$$\begin{aligned} E(\mathbf{r}, t) &= \sum_m \int d\omega E_m(\omega) g_m(\omega; \mathbf{r}, t) \\ &= \sum_m \int d\omega a_m(\omega) \exp[i\phi_m(\omega)] \exp\left\{-i\omega\left[(t - t_m) - \frac{r}{c}\right]\right\} \end{aligned} \quad (1)$$

Here, a point-to-point propagation in vacuum with speed of  $c$  is assumed. In Eq. (1),  $E_m(\omega)$  is the spectral amplitude density of the  $m$ th subfield and  $g_m(\omega; r, t)$  is the Green's function or phase propagator that propagates the  $m$ th subfield from the  $m$ th point-like sub-source to space-time coordinates  $(\mathbf{r}, t)$ . The spectral amplitude density, being a complex quantity, can be separated into a real amplitude  $a_m(\omega)$  and an initial phase factor  $e^{i\phi_m(\omega)}$  as  $E_m(\omega) = a_m(\omega)e^{i\phi_m(\omega)}$ . If we introduce a detuning frequency:  $\nu = \omega - \omega_0$  with  $\omega_0$  being the central frequency of the subfield, then the  $m$ th wave packet is calculated as follows:

$$\begin{aligned} E_m(\mathbf{r}, t) &= \exp\left[-i\omega_0\left(t - t_m - \frac{r}{c}\right) + i\phi_{0m}\right] \int_{-\infty}^{\infty} d\nu a_m(\nu) \exp\left[-i\nu\left(t - t_m - \frac{r}{c}\right)\right] \\ &= \exp\left[-i(\omega_{0m}\tau_m - \phi_{0m})\right] \mathcal{F}_{\tau_m}[a_m(\nu)] \end{aligned} \quad (2)$$

where  $\tau \equiv t - r/c$  and  $\tau_m = \tau - t_m$ . The function  $a_m(\nu)$  describes the amplitude as a function of the frequencies present in the  $m$ th subfield and the infinite integral represents the coherent superposition of all of these frequency modes. We can label this Fourier transform as a wave packet which propagates through space and time. For mathematical simplicity, the rest of this paper assumes that the linewidth of each frequency band is infinitesimally narrow, i.e.  $\Delta\nu \sim 0$ . In this limit, the spectral distribution function  $a_m(\nu)$  is approximated as a  $\delta$ -function, positioned at  $\omega_0$ , and the integral gives a constant. In reality, the linewidth is always constrained by a minimum quantum uncertainty in the atomic transition, hence impacting their temporal coherence.

By definition, the measured intensity at point  $(\mathbf{r}, t)$  is calculated as the magnitude squared of the total electric field at  $(\mathbf{r}, t)$ :

$$\langle I(\mathbf{r}, t) \rangle = \left\langle \sum_{m,n} E_m(\mathbf{r}, t) E_n^*(\mathbf{r}, t) \right\rangle = \left\langle \sum_{m=n} |E_m(\mathbf{r}, t)|^2 \right\rangle + \left\langle \sum_{m \neq n} E_m(\mathbf{r}, t) E_n^*(\mathbf{r}, t) \right\rangle \quad (3)$$

where the sum over  $m$  ( $n$ ) includes all subfields present at  $(\mathbf{r}, t)$ . In the limit of the ensemble average, which involves the summing of all possible realizations of the subfields, the second term vanishes due to the superposition of all possible random phases  $\phi_{0m}$  and  $\phi_{0n}$  associated with the subfields. However, if only a finite number of subfields contribute to the measurement, the  $m \neq n$  term may not vanish and can be observable from the measurement with a photodetector. In such case, it is identified as the intensity fluctuation, and is usually considered “noise” in the measurement of  $\langle I(\mathbf{r}, t) \rangle$ . Thus, for a large number of randomly created, overlapping and partially overlapping wave packets, the only *stable* interference is the interference in which the  $m$ th subfield or wave packet is interfering with itself, the  $m = n$  term in Eq. (3), due to the cancellation of the initial phase information. Interference between different subfields or wave packets, although technically present all the time, varies fast and in a random fashion, and hence becomes unobservable after the ensemble average. This is true for a thermal source which we will be focusing on; however, for a source of coherent radiation, all subfields have the same initial phase,  $\phi_{0m}$ , so there are no random phases differences present to produce these intensity fluctuations.

## 2.2. Two-photon interference

Before examining two-photon optical beats, it is worth highlighting the implications of quantum theory of optical coherence which suggests that the subfield in Einstein's granularity model

of light is equivalent to the *effective wavefunction* of photon in Glauber's theory [1,5,16,17]. Based on this connection, the second-order coherence function can be defined in terms of either intensity-intensity correlation or photon number correlation, jointly measured by two point-like photodetectors  $D_1$  and  $D_2$ . It is possible that for a thermal source composed of a large ensemble of sub-sources, each of the field-wise contribution to the correlation can be a different subfield. If such a joint-photodetection event occurs at space-time coordinates  $(\mathbf{r}_1, t_1)$  and  $(\mathbf{r}_2, t_2)$ , the calculation of second-order coherence function [17] of thermal field follows from Einstein's picture of radiation as

$$\begin{aligned} \Gamma^{(2)}(\mathbf{r}_1, t_1; \mathbf{r}_2, t_2) &= \langle E^*(\mathbf{r}_1, t_1)E(\mathbf{r}_1, t_1)E^*(\mathbf{r}_2, t_2)E(\mathbf{r}_2, t_2) \rangle \\ &= \left\langle \sum_{m,n,p,q} E_m^*(\mathbf{r}_1, t_1)E_n(\mathbf{r}_1, t_1)E_p^*(\mathbf{r}_2, t_2)E_q(\mathbf{r}_2, t_2) \right\rangle \end{aligned} \quad (4)$$

where the radiation fields are written as superposition of the subfields in Einstein model. Here, the self-correlation terms at each detector,  $m = n$  and  $p = q$ , survive the averaging process whereas the terms that still have a random phase attributed to them average to zero after summing over all possible random phases. However, in the specific case of  $p = n$  and  $q = m$ , the random phases also cancel out, and the following terms survive from the ensemble average, or the expectation evaluation:

$$\begin{aligned} \Gamma^{(2)}(\mathbf{r}_1, t_1; \mathbf{r}_2, t_2) &= \sum_m E_m^*(\mathbf{r}_1, t_1)E_m(\mathbf{r}_1, t_1) \sum_n E_n^*(\mathbf{r}_2, t_2)E_n(\mathbf{r}_2, t_2) \\ &+ \sum_{m \neq n} E_m^*(\mathbf{r}_1, t_1)E_n(\mathbf{r}_1, t_1)E_n^*(\mathbf{r}_2, t_2)E_m(\mathbf{r}_2, t_2) \\ &= \langle I(\mathbf{r}_1, t_1) \rangle \langle I(\mathbf{r}_2, t_2) \rangle + \langle \Delta I(\mathbf{r}_1, t_1) \Delta I(\mathbf{r}_2, t_2) \rangle \end{aligned} \quad (5)$$

where the indices of the self-correlation at  $D_2$  have been relabeled as  $n$ . In Eq. (5), the first term corresponds to a product of the mean intensities measured by the detectors placed at  $(\mathbf{r}_1, t_1)$  and  $(\mathbf{r}_2, t_2)$ , while the second term is the intensity fluctuation correlation (IFC) measured by them jointly. For spatially incoherent thermal radiation, the first term is a constant but the second-term is nontrivial. In those cases, the measurement of second-order coherence function of thermal field may still contain useful information from the correlation of the intensity fluctuations measured at the pair of detectors [18]. As described earlier, the basis for such correlation is two-photon interference.

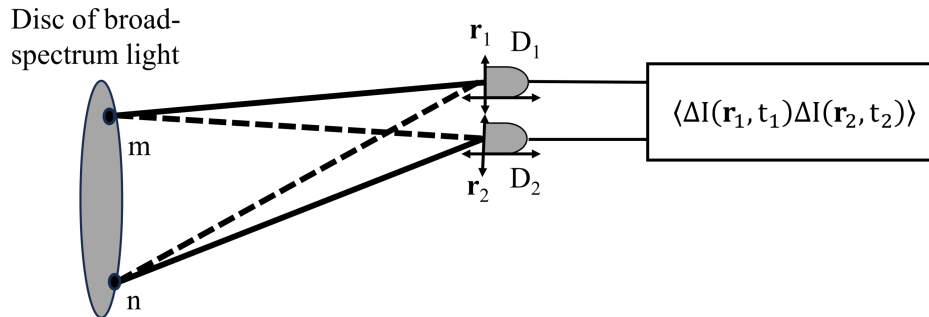


**Fig. 1.** Conceptual sketch of interference between two-photon amplitudes [1]. The solid and dashed lines are being used as visual tools to denote two alternative paths for subfields.

As shown in Fig. 1, two-photon interference can be visualized as a superposition of two alternative pathways of subfields. Here, two incoherent sub-sources within a larger ensemble, labeled  $m$  and  $n$ , respectively are considered. The subfields  $E_m, E_n$  created from them are assumed to have the same central frequency and are emitted randomly at different times. A joint detection of the subfields by two point-like detectors  $D_1$  and  $D_2$ , which can be scanned along different spatial dimensions, occurs as a consequence of constructive superposition of these pathways.

### 3. Multi-band two-photon interference with slow detectors

In the Hanbury Brown and Twiss (HBT)-type measurement of Fig. 2, we suppose two sets of incoherent sub-sources, labeled  $m$  and  $n$ , respectively, and the subfields created from  $m$ ,  $m = 1, 2, 3, \dots$  at different times, have a Red spectrum and the subfields created from  $n$ ,  $n = 1, 2, 3, \dots$  at different times, have a Green spectrum. As was mentioned earlier, each subfield emitted from these sub-sources are assumed to have an infinitesimally narrow bandwidth. Each subfield ending up at either of the two point-like detectors  $D_1$  at  $(x_1, t_1)$  and  $D_2$  at  $(x_2, t_2)$  can be considered to be a superposition between two distinct yet indistinguishable amplitudes, one visualized with solid and the other with dotted lines. The interference between these probability amplitudes is what gives rise to the two-photon interference in which the intensity fluctuation correlation (IFC) is the nontrivial part. So, the intensity fluctuation correlation term, defined in Eq. (5), assumes the form:

$$\langle \Delta I(x_1, t_1) \Delta I(x_2, t_2) \rangle = \frac{1}{4} \sum_{m \neq n} E_m^*(x_1, t_1) E_n^*(x_2, t_2) E_n(x_1, t_1) E_m(x_2, t_2) \quad (6)$$

When the source of radiation contains two dominant frequencies, which we will label as  $\omega_{0R}$  and  $\omega_{0G}$  corresponding to red and green colors respectively, then each individual subfield emitted by the source could either be quasi-monochromatic (red or green) or every subfield could be in a coherent superposition of both frequencies (red and green). For the purpose of our derivation, we will exclusively consider the former case and assume that the point detectors we are dealing with are sensitive to both frequencies. As can be seen from Eq. (5), the correlation between the two detectors is a result of joint detection of only two photons (the  $m$ th and  $n$ th) at a time. This implies that we have four possible pairings of frequencies:  $m$  is red while  $n$  is also red,  $m$  is green while  $n$  is also green,  $m$  is red while  $n$  is green, and  $m$  is green while  $n$  is red. Thus, the total intensity fluctuation correlation for a thermal source emitting red and green colors will be the following expression:

$$\begin{aligned} \langle \Delta I(x_1, t_1) \Delta I(x_2, t_2) \rangle_{\text{total}} &= \langle \Delta I(x_1, t_1) \Delta I(x_2, t_2) \rangle_{RR} + \langle \Delta I(x_1, t_1) \Delta I(x_2, t_2) \rangle_{GG} + \langle \Delta I(x_1, t_1) \Delta I(x_2, t_2) \rangle_{RG} \\ &\quad + \langle \Delta I(x_1, t_1) \Delta I(x_2, t_2) \rangle_{GR} \end{aligned} \quad (7)$$

This expression implicitly consists of optical beats as a function of spatio-temporal variables. However, these terms are subject to the time averaging effects of detectors. For “slow” detectors, the uncertainty of the relative registration time  $\delta(t_1 - t_2)$  erases “fast” optical beats due to the averaging and we are left with

$$\begin{aligned} \langle \Delta I(x_1, t_1) \Delta I(x_2, t_2) \rangle_{\text{total}} &= \int_{\Delta T} d(t_1 - t_2) \left[ \langle \Delta I(x_1, t_1) \Delta I(x_2, t_2) \rangle_{RR} \right. \\ &\quad \left. + \langle \Delta I(x_1, t_1) \Delta I(x_2, t_2) \rangle_{GG} \right] \end{aligned} \quad (8)$$

While not an issue with ideal/fast detectors, it is worthwhile to mention that the amplitude of IFC will drop as more frequency bands are considered for such measurement. For a two-band

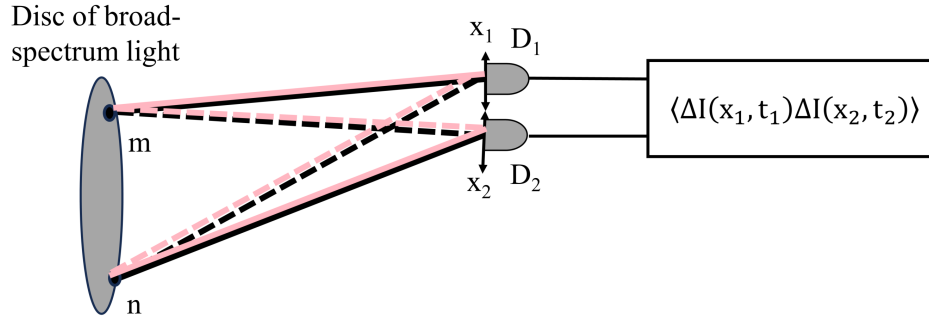


**Fig. 2.** Conceptual sketch of interference between two-photon amplitudes in a double-slit interferometer. Similar to Fig. 1, the solid and dashed lines are being used as visual tools to denote two alternative paths for subfields. Since the source emits subfields of two different frequencies or color, each of the two alternative pathways is shown to have two lines corresponding to different colors.

case such as the above, the amplitude of the IFC measured with slow detectors can drop by an additional factor of 50%. In general, for an  $N$ -band thermal source, the measured IFC can get reduced by  $1/N$ .

This multi-band interference has important implications for two-photon beats and multi-band two-photon imaging, which are discussed next.

### 3.1. Two-photon beats in Young's double-slit interferometer

Figure 3 shows a typical double-slit interferometer setup. The thermal source illuminating the interferometer is modeled as a large ensemble of incoherent sub-sources, labeled  $m$  ( $n$ ). As was mentioned earlier, each subfield emitted from these sub-sources are assumed to have an infinitesimally narrow bandwidth. For the purpose of these calculations, the mid-point between the two slits is defined to be the origin of the coordinate system and the slits are assumed to be infinitesimally narrow such that the effects of diffraction may be ignored. Furthermore, we consider a far-field approximation to write the expression for propagators in our calculations. Each subfield ending up at either of the two point-like detectors  $D_1$  at  $(x_1, t_1)$  and  $D_2$  at  $(x_2, t_2)$  can be considered to be a superposition between  $A$ -path and  $B$ -path amplitudes, where  $A$  and  $B$  denote the slit positions  $x_A, x_B$ , as shown in Fig. 3. So, the intensity fluctuation correlation term, defined in Eq. (5), assumes the form:

$$\begin{aligned} & \langle \Delta I(x_1) \Delta I(x_2) \rangle \\ &= \frac{1}{4} \sum_{m \neq n} [E_{mA}(x_1) + E_{mB}(x_1)]^* [E_{nA}(x_2) + E_{nB}(x_2)]^* \\ & \quad \times [E_{nA}(x_1) + E_{nB}(x_1)] [E_{mA}(x_2) + E_{mB}(x_2)] \end{aligned} \quad (9)$$

where we have used the notations  $E_{mA}(x_1) = E_m(x_A)E_A(x_1)$ , etc. Our calculations have shown that the IFC contributed by the “bichromatic” RG+GR combinations is

$$\begin{aligned} & \langle \Delta I(x_1, t_1) \Delta I(x_2, t_2) \rangle_{RG} + \langle \Delta I(x_1, t_1) \Delta I(x_2, t_2) \rangle_{GR} \\ &= 2I_0^2 \left[ \cos \left[ \frac{\omega_{0R}d}{2cz} (x_1 - x_2) \right] + \text{sinc} \left( \frac{\omega_{0R}d\Delta\theta_s}{2c} \right) \cos \left[ \frac{\omega_{0R}d}{2cz} (x_1 + x_2) \right] \right] \left[ \cos \left[ \frac{\omega_{0G}d}{2cz} (x_1 - x_2) \right] \right. \\ & \quad \left. + \text{sinc} \left( \frac{\omega_{0G}d\Delta\theta_s}{2c} \right) \cos \left[ \frac{\omega_{0G}d}{2cz} (x_1 + x_2) \right] \right] \cos \left[ (\omega_{0G} - \omega_{0R})(t_1 - t_2 - \frac{x_1^2 - x_2^2}{2cz}) \right] \end{aligned} \quad (10)$$



As can be seen, it consists of optical beats as a function of spatio-temporal variables. This means, for the RG+GR combinations, fast detectors that guarantee  $\delta(t_1 - t_2) < 2\pi/(\omega_{0G} - \omega_{0R})$ , would be necessary for the observation of corresponding optical beats in the intensity fluctuation correlation measurement. However, the IFC contributed by the quasi-monochromatic RR+GG combinations is

$$\begin{aligned}
 & \langle \Delta I(x_1) \Delta I(x_2) \rangle_{RR} + \langle \Delta I(x_1) \Delta I(x_2) \rangle_{GG} \\
 &= 2I_0^2 \left\{ 1 + \cos \left[ \frac{(\omega_{0R} + \omega_{0G})d}{2cz} (x_1 - x_2) \right] \cos \left[ \frac{(\omega_{0G} - \omega_{0R})d}{2cz} (x_1 - x_2) \right] \right. \\
 &\quad + 2 \text{sinc} \left( \frac{\omega_{0R} d \Delta \theta_s}{2c} \right) \cos \left[ \frac{\omega_{0R} d}{2cz} (x_1 - x_2) \right] \cos \left[ \frac{\omega_{0R} d}{2cz} (x_1 + x_2) \right] \\
 &\quad + 2 \text{sinc} \left( \frac{\omega_{0G} d \Delta \theta_s}{2c} \right) \cos \left[ \frac{\omega_{0G} d}{2cz} (x_1 - x_2) \right] \cos \left[ \frac{\omega_{0G} d}{2cz} (x_1 + x_2) \right] \\
 &\quad + \text{sinc}^2 \left( \frac{\omega_{0R} d \Delta \theta_s}{2c} \right) \cos^2 \left[ \frac{\omega_{0R} d}{2cz} (x_1 + x_2) \right] \\
 &\quad \left. + \text{sinc}^2 \left( \frac{\omega_{0G} d \Delta \theta_s}{2c} \right) \cos^2 \left[ \frac{\omega_{0G} d}{2cz} (x_1 + x_2) \right] \right\}, \quad (11)
 \end{aligned}$$

for which a more detailed derivation of the quasi-monochromatic case can be found in Ref. [10]. Eq. (11) clearly demonstrates the presence of optical beats with a beat frequency  $\omega_{0G} - \omega_{0R}$  resulting from the superposition of distinct two-photon interference patterns originating from each color. Because this result is exclusively the combination of two monochromatic interference terms, it is free of any time averaging effects of the detectors, thus ensuring the possibility of the measurement of beat frequency with slow detectors. A quick inspection of the expression in Eq. (11) suggests that the contribution (or visibility) of certain cosine functions depends on the angular size of the source. When the radiation field is spatially incoherent, i.e., in the limiting case of  $d \gg \frac{c}{\omega_{0R} \Delta \theta_s}$ , the total IFC results in:

$$\langle \Delta I(x_1) \Delta I(x_2) \rangle_{\text{total}} = 2I_0^2 \left\{ 1 + \cos \left[ \frac{(\omega_{0R} + \omega_{0G})d}{2cz} (x_1 - x_2) \right] \cos \left[ \frac{(\omega_{0G} - \omega_{0R})d}{2cz} (x_1 - x_2) \right] \right\} \quad (12)$$

Clearly, this result implies that even under the condition of full spatial incoherence, the two-photon interference does not vanish. Therefore, the beat term resulting from the superposition of two distinct interference patterns related to the two colors is still retained. The result of Eq. (12) is compared with two entirely monochromatic cases in the example plot shown in Fig. 4. As has been shown, the measurement of two-photon interference in a double-slit interferometer is turbulence-resistant for the monochromatic case [9,10]. The calculations presented here represent the superposition of two such interference patterns for different colors and are expected to be turbulence-resistant when similar experimental conditions are maintained. This is based on the premise that although the index of refraction (and thus turbulence) for red color could be slightly different from that for green, the total measurable IFC is a result of red interfering with red and green interfering with green and hence, so neither of these two cases experiences dispersion effects, i.e., both are turbulence-resistant in the same way as the monochromatic case.

### 3.2. Multi-band imaging via joint detection of two-photon beats

The result above begs us to explore the potential of imaging with multi-band source and slow detectors. So far, we have considered a standalone double-slit interferometer and a distant source of incoherent thermal radiation. One can also model the source as being an ensemble of a very large number of “double-slits”. This can be visualized by taking infinitesimally thin strips of point sources and taking a parallelly aligned pair of such strips at a time to calculate the IFC. For the total IFC, the result can be integrated over the size of the source such that the separation of



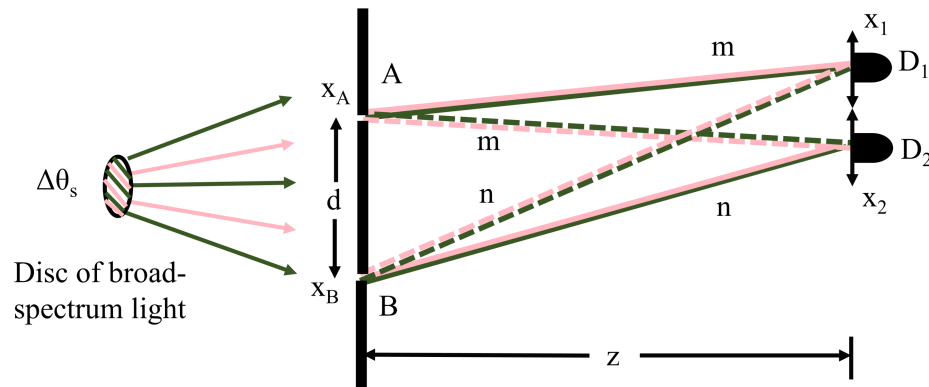


**Fig. 3.** Conceptual sketch of interference between two-photon amplitudes in a double-slit interferometer. Similar to Fig. 1, the solid and dashed lines are being used as visual tools to denote two alternative paths for subfields. Since the source emits subfields of two different frequencies or color, each of the two alternative pathways is shown to have two lines corresponding to different colors.

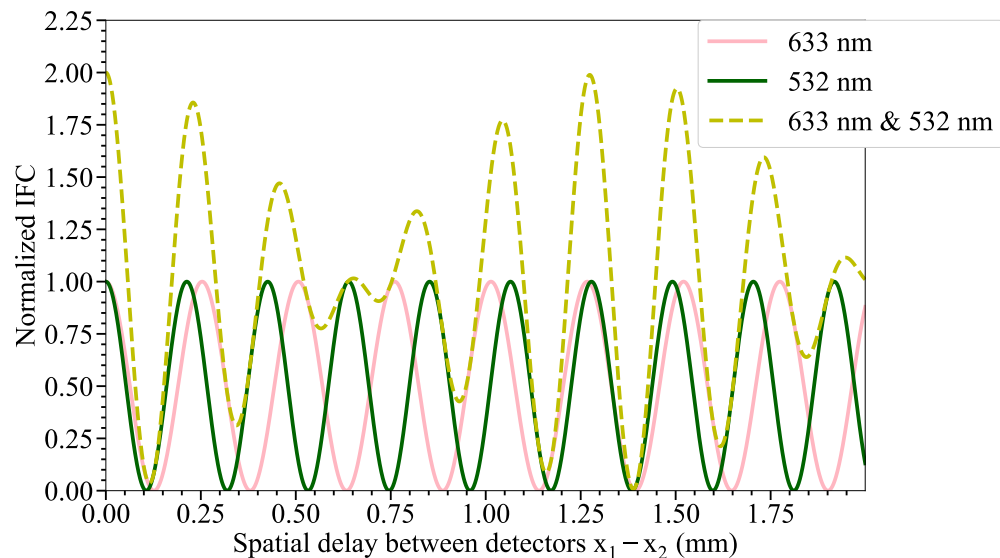


**Fig. 4.** Theoretical plot demonstrating normalized two-photon interference patterns for two different colors of light and the optical beats resulting from their superposition. Specific cases of red and green colors with wavelengths 633 nm and 532 nm, respectively, are considered. It can be seen that the amplitude of the beat pattern is the sum of the normalized IFC for each color of light. For this analytical example we have taken the slit width to be infinitesimally narrow, slit separation to be 2.5 mm, and the observation plane to be 1 m away from the slits.

the slits varies from zero to the source diameter. On the detector end of the calculations, one can consider a typical ghost imaging setup as shown in Fig. 5, and get the point-to-point correlation between the object and ghost image planes.

In this setup, the subfields emitted by the point-like subsources have equal probabilities of giving off different colors (for ease of calculations, we consider a two-color source for now). The

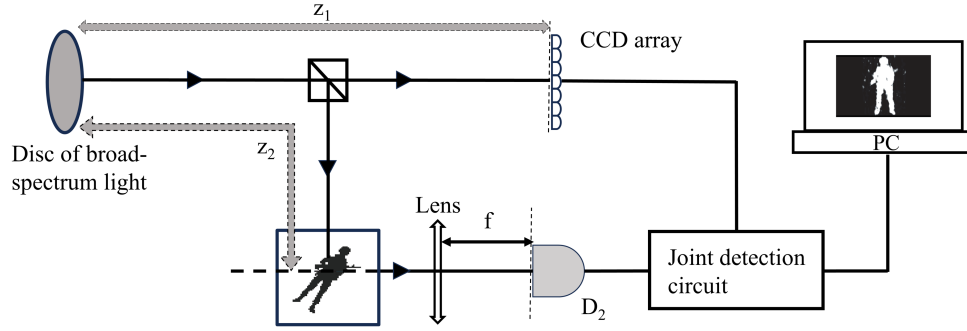


**Fig. 5.** Conceptual sketch of ghost imaging with multi-band thermal source via joint detection with slow detectors. The setup is a typical ghost imaging scheme with thermal source [1].

object plane ( $\rho_o$ ), the bucket detector plane ( $\rho_2$ ), and the image plane ( $\rho_i = \rho_1$ ) are in the far-field at distances  $z_2$  and  $z_1$ , respectively. One can consider  $z_1 = z_2$  for simplicity. The bucket detector is placed at the focal length  $f$  of the lens. As before, there are four combinations of colors that can constitute a two-photon pair; and two of these combinations do not survive the time averaging caused by slow detectors. The result, then, is that the IFC between these two planes is

$$\begin{aligned}
 & \langle \Delta I(\rho_1) \int d\rho_2 \Delta I(\rho_2) \rangle_{RR} + \langle \Delta I(\rho_1) \int d\rho_2 \Delta I(\rho_2) \rangle_{GG} \\
 &= \left[ \sum_{m \neq n} E_m^*(r_1, t_1) E_n(r_1, t_1) \int d\rho_2 E_n^*(r_2, t_2) E_m(r_2, t_2) \right]_{RR} \\
 &+ \left[ \sum_{m \neq n} E_m^*(r_1, t_1) E_n(r_1, t_1) \int d\rho_2 E_n^*(r_2, t_2) E_m(r_2, t_2) \right]_{GG} \\
 &\propto \int d\rho_o |A(\rho_o)|^2 \otimes \text{somb}^2 \left[ \frac{\omega_{0R} \Delta \theta_s}{2c} |\rho_1 - \rho_o| \right] \\
 &+ \int d\rho_o |A(\rho_o)|^2 \otimes \text{somb}^2 \left[ \frac{\omega_{0G} \Delta \theta_s}{2c} |\rho_1 - \rho_o| \right]
 \end{aligned} \quad (13)$$

This result shows a point-spread correlation function between the image and the object planes, with two-photon beats at the heart of the correlation. For a multi-band source, the IFC will be a sum of the convolutions in Eq. (13) for different central frequencies.

We can approximate the point-spread  $\text{somb}^2$ -functions as point-to-point delta functions for a source with large angular diameter, and in this case, both the RR and GG contributions are identical:

$$\langle \Delta I(\rho_1) \int d\rho_2 \Delta I(\rho_2) \rangle \propto \int d\rho_o |A(\rho_o)|^2 \delta(\rho_1 - \rho_o) = |A(\rho_1)|^2 \quad (14)$$

The point-spread function is loosely dependent on the pixel size of the CCD array being used. For this to be considered point-to-point delta function, it is a sufficient condition that the point-spread function be narrower than the size of an individual pixel.

It should be emphasized that the result derived above is not only of fundamental importance, but also has implications for applied fields such as in second-order imaging with thermal radiation source. In particular, the point-to-point correlations deduced from the measurement of optical beats presented in this work could potentially be extended to realize the well-known ghost imaging [1] or high resolution astronomical imaging via intensity interferometry [19,20] for multi-band sources. As the two-photon beats are turbulence-resistant, the IFC itself can be resistant to the detrimental effects of turbulence. Moreover, generalizing the idea of narrow slits

of the double-slit interferometer discussed here may find interesting applications in quantum information processing and astrophysical measurements when each of the two slits can be modeled by two atoms [21], two molecules [22] or even the components of a binary star [23] that emit two different colors or frequency bands.

#### 4. Conclusion

The findings reported in this work suggest that optical measurement techniques involving multi-band source can be realized with “slow” detectors via the measurement of two-photon beats. The underlying two-photon beats represent a two-photon interference phenomenon: a pair of randomly created and randomly paired photons interfering with the pair itself. Specifically, we showed that the concept of multi-band two-photon interference can be directly applied to two-photon beats with an incoherent source in a double-slit interferometer, and the possibility of multi-band ghost imaging of multi-band, incoherent thermal light. Both schemes enable us to observe two-photon beats in the second-order correlation measurement, which depend only on the spatial coordinates of the detectors and not on the photodetection times. Building upon earlier studies of turbulence-resistant two-photon interference, it is also found that the observation of two-photon beats can be free from the detrimental effects of turbulence, and consequently the multi-band imaging scheme is also turbulence-resistant. Notably, these findings are not only of fundamental importance, but also have implications for applied fields such as in second-order imaging with thermal radiation source, quantum information and astrophysical measurements.

**Funding.** Northrop Grumman Corporation.

**Disclosures.** The authors declare no conflicts of interest.

**Data availability.** No data were generated or analyzed in the presented research.

#### References

1. Y. Shih, *An Introduction to Quantum Optics: Photon and Biphoton Physics* (CRC press, Taylor & Francis, 2021).
2. R. H. Brown and R. Q. Twiss, “Correlation between photons in two coherent beams of light,” *Nature* **177**(4497), 27–29 (1956).
3. R. H. Brown and R. Q. Twiss, “A test of a new type of stellar interferometer on sirius,” *Nature* **178**(4541), 1046–1048 (1956).
4. U. Fano, “Quantum theory of interference effects in the mixing of light from phase-independent sources,” *Am. J. Phys.* **29**(8), 539–545 (1961).
5. R. Loudon, *The Quantum Theory of Light* (Oxford University Press, 2000).
6. F. S. Crawford Jr., *Waves* (McGraw-Hill, 1968).
7. W. Martienssen and E. Spiller, “Coherence and Fluctuations in Light Beams,” *Am. J. Phys.* **32**(12), 919–926 (1964).
8. G. Scarcelli, A. Valencia, and Y. Shih, “Two-photon interference with thermal light,” *Europhys. Lett.* **68**(5), 618–624 (2004).
9. T. A. Smith and Y. Shih, “Turbulence-free double-slit interferometer,” *Phys. Rev. Lett.* **120**(6), 063606 (2018).
10. T. A. Smith and Y. Shih, “Turbulence-free two-photon double-slit interference with coherent and incoherent light,” *Opt. Express* **27**(23), 33282–33297 (2019).
11. N. Bobroff, “Residual errors in laser interferometry from air turbulence and nonlinearity,” *Appl. Opt.* **26**(13), 2676–2682 (1987).
12. H. T. Yura, “Mutual coherence function of a finite cross section optical beam propagating in a turbulent medium,” *Appl. Opt.* **11**(6), 1399–1406 (1972).
13. A. Einstein, “Über einen die Erzeugung und Verwandlung des Lichtes betreffenden heuristischen Gesichtspunkt [adP 17, 132 (1905)],” *Ann. Phys.* **517**(S1), 164–181 (2005).
14. A. Einstein and L. Hopf, “Über einen Satz der Wahrscheinlichkeitsrechnung und seine Anwendung in der Strahlungstheorie [adP 33, 1096 (1910)],” *Ann. Phys.* **517**(S1), 347–356 (2005).
15. A. Einstein, “Antwort auf eine Abhandlung M.v. Laues Ein Satz der Wahrscheinlichkeitsrechnung und seine Anwendung auf die Strahlungstheorie [adP 47, 879 (1915)],” *Ann. Phys.* **517**(S1), 509–516 (2005).
16. M. O. Scully and M. S. Zubairy, *Quantum Optics* (Cambridge University Press, 1997).
17. R. J. Glauber, “The quantum theory of optical coherence,” *Phys. Rev.* **130**(6), 2529–2539 (1963).
18. J. W. Goodman, *Statistical Optics* (John Wiley & Sons, 2015).
19. D. Dravins, T. Lagadec, and P. D. Nuñez, “Optical aperture synthesis with electronically connected telescopes,” *Nat. Commun.* **6**(1), 6852 (2015).

20. A. U. Abeysekara, W. Benbow, and A. Brill, "Demonstration of stellar intensity interferometry with the four veritas telescopes," *Nat. Astron.* **4**(12), 1164–1169 (2020).
21. A. Neuzner, M. Körber, and O. Morin, "Interference and dynamics of light from a distance-controlled atom pair in an optical cavity," *Nat. Photonics* **10**(5), 303–306 (2016).
22. H. Zhou, W. E. Perreault, N. Mukherjee, *et al.*, "Quantum mechanical double slit for molecular scattering," *Science* **374**(6570), 960–964 (2021).
23. R. H. Brown, R. Q. Twiss, and A. C. B. Lovell, "Interferometry of the intensity fluctuations in light III. applications to astronomy," *Proc. R. Soc. Lond. A* **248**(1253), 199–221 (1958).